Journal of ELECTRICAL ENGINEERING, VOL. 62, NO. 1, 2011, 37–43

SWITCHING MAGNETIZATION MAGNETIC FORCE MICROSCOPY — AN ALTERNATIVE TO CONVENTIONAL LIFT–MODE MFM

Vladimír Cambel [*] — **Dagmar Gregušová** [*] — **Peter Eliáš** [*] — **Ján Fedor** [*] — **Ivan Kostič** [**] — **Ján Maňka** [***] — **Peter Ballo** [****]

In the paper we present an overview of the latest progress in the conventional lift-mode magnetic force microscopy (MFM) technique, achieved by advanced MFM tips and by lowering the lift height. Although smaller lift height offers improved spatial resolution, we show that lowered tip-sample distance mixes magnetic, atomic and electric forces. We describe an alternative to the lift-mode procedure - Switching Magnetization Magnetic Force Microscopy [SM-MFM], which is based on two-pass scanning in tapping mode AFM with reversed tip magnetization between the scans. We propose design and calculate the magnetic properties of such SM-MFM tips. For best performance the tips must exhibit low magnetic moment, low switching field, and single-domain state at remanence. The switching field of such tips is calculated for Permalloy hexagons.

K e y w o r d s: magnetic force microscopy, micromagnetic calculations, switching field

1 INTRODUCTION

Scanning probe magnetic force microscopy (MFM) [2, 3] is the state-of-the-art tool used to explore submicron magnetic domain structures and written bit patterns in recording media [4, 5], for imaging of currents in internal conductors [6], *etc.* MFM is popular for its high spatial resolution (~ 50 nm), high sensitivity in large variety of environmental conditions, and for simple sample preparation.

MFM uses various procedures for different samples: constant height mode, constant frequency shift mode [7] or combined tapping/lift mode [8]. For atomically flat samples the constant height mode can be used the tip scans across the surface at a predetermined height while the cantilever frequency shift is monitored. In the constant frequency shift mode a feedback adjusts the tip-sample distance in order to keep the cantilever frequency constant. The last method is a two-pass one, developed to distinguish the magnetic and non-magnetic interactions. Within the first pass the tip scans the sample topology in the tapping mode. Magnetic forces are mapped in the second pass during which influences of atomic forces are suppressed by lifting the tip off the surface to the constant offset (lift) distance over it.

The spatial resolution is dominantly defined by the tip radius and the tip-sample separation [4]. For good magnetic-and-nonmagnetic forces separation the lift height $\sim$30–50 nm is commonly selected.

Recently, a large number of nanomagnetic devices have been developed — spin electronic devices, perpendicular magnetic storage media, and magnetic random access memories [9–11]. In such memories the minimal bit length is expected to be well below 20 nm [12], so improved spatial resolution in MFM technique below 10 nm is clearly needed. Moreover, MFM response is often sufficiently sensitive for qualitative characterization of the micromagnetic properties of a sample, such as hard or soft magnetic properties [13, 14], but quantitative interpretation of MFM signal is remains a difficult task. In some cases it can be determined theoretically from the convolution of the sample magnetization and the tip stray field [15]. In that case the knowledge of precise tip stray field can be used to determine the sample magnetization [16–18]. The experiments have shown that the tip calibration is difficult to obtain, and the tip moment is impossible to maintain during scanning.

Several attempts have been done to increase the MFM space resolution using specially fabricated MFM tips. N. Yoshida *et al* [19] and H. Kuramochi *et al* [20] evaporated ferromagnetic material directly onto the carbon-nanotube (CNT) tips and presented improved spatial resolution and lower invasiveness of such probes. M.R. Koblishka *et al* [21] and S. Huang *et al* [22] milled standard MFM tips and prepared high-aspect-ratio tips using focused ion beam (FIB). L. Folks *et al* [23] applied the FIB milling to increase the MFM lateral resolution and magnetic sensitivity. Recently, F. Wolny [24] fabricated MFM tip by filling CNT with ferromagnetic iron.

Such MFM tips show two negative features: first, the fabrication is difficult and needs separate micromachining of each individual tip. Therefore, the magnetic properties of each tip differ, their mass production is difficult to achieve, and their final price is very high. Second, to increase the spatial resolution, the tips operate at a distance at which the force mixing is significant and then

Institute of Electrical Engineering, vladimir.cambel@savba.sk; [**] Institute of Informatics; [***] Institute of Measurement Science, Slovak Academy of Sciences, Dúbravská cesta 9, 841 04 Bratislava, Slovakia, [****] Slovak University of Technology, Faculty of Electrical Engineering and Information technology, Ilkovičova 3, 812 19 Bratislava, Slovakia

DOI: 10.2478/v10187-011-0006-2, ISSN 1335-3632 © 2011 FEI STU

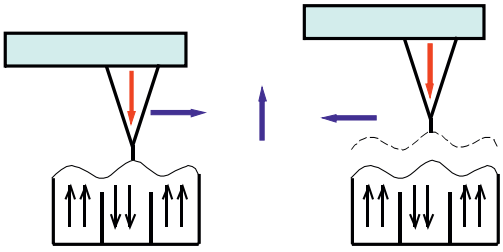

Fig. 1. Conventional MFM scanning method — two pass technique. Within the first pass van der Waals forces are scanned, then is the tip lifted to the lift distance, in which the magnetic forces are scanned

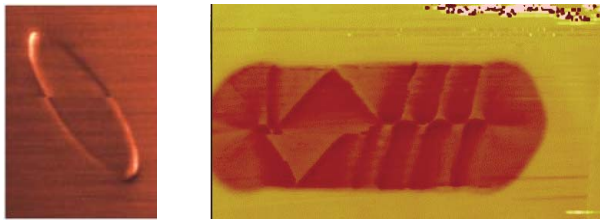

Fig. 2. Invasiveness of MFM scanning. Left figure shows single-domain Py ellipse switched by the MFM tip to the opposite polarity while scanning the upper part of it; right figure shows magnetic domain pattern switched to a more stable state while scanning the central part of the Py sample.

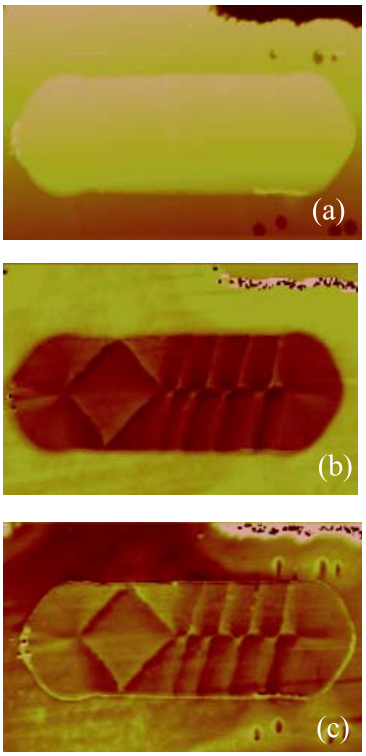

Fig. 3. Permalloy object placed on the top of the Hall probe, (a) topography, (b) MFM scan of magnetic domains for zero bias current in the probe, (c) MFM scan gives a mixture of magnetic, electrostatic and atomic forces if current is flowing in the probe from bottom to the top

the separation of the signal into magnetic, electric and atomic forces is impossible.

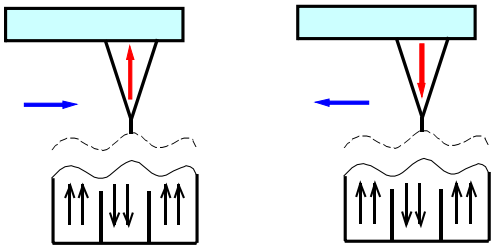

Fig. 4. SM-MFM principle. Both scans are done in the tapping mode, but the tip magnetization (vertical arrow in the tip) is reversed between them. The addition of the signals gives atomic and electric forces, their difference are clear magnetic forces

We compare the standard MFM technique with the new one, called Switching Magnetization MFM (SM-MFM) [1]. The technique is based on two passes in the tapping mode with the tip magnetization reversed between them. The sum of the collected traces obtained with opposite tip magnetization represents the mixture of atomic and electrostatic forces. On the other hand, the trace difference corresponds to clear magnetic forces.

2 RESULTS AND DISCUSSIONS

2.1 Tapping/lift-mode MFM — invasive and force-mixing method

Figure 1 shows the tapping/lift MFM method. Within the first pass the tip scans the sample surface in the tapping mode. In the second pass the tip is lifted off the surface to the lift distance, and the magnetic forces are scanned via the evaluation of the frequency or phase shift of the cantilever. The lift distance (and the resolution) of the method is typically 50 nm. The distance separates effectively the magnetic forces from the van der Waals ones.

The effects of tip invasiveness and force mixing are reported in Fig. 2, in which two examples are shown. Left part shows single domain Permalloy (Py) ellipse switched by the tip to the opposite polarity while scanning the upper part of it. Right part shows the magnetic domain pattern that consists of diamond and cross-tie structures switched to a more stable state while the tip was scanning the ellipse central part. Lift distance in both cases was 50 nm. Recently, also opposite effect was observed — the sample's magnetization have changed the magnetic moment of the metal-coated tip [25, 26].

Reduced scanning distance leads to collection of the force signal that is a mixture of magnetic, atomic, and electric forces. Figure 3 shows a Py object placed on a Hall probe and scanned by the MFM tapping/lift method at the lift distance of 50 nm. Figure 3(a) depicts the sample's topography obtained within the first pass (tapping mode). Figures 3(b) and 3(c) are the MFM scans of the object within the lift mode for a zero and non-zero bias currents in the Hall probe, respectively. In the case (b)

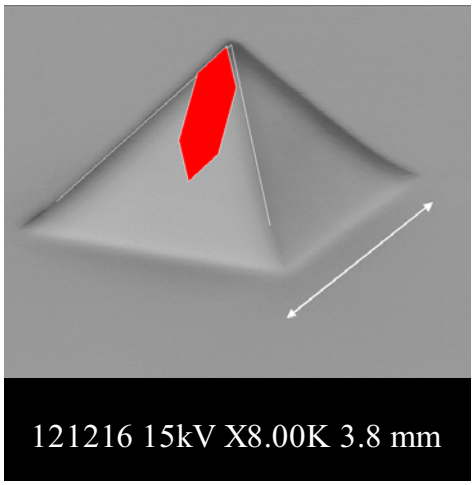

Fig. 5. Side view on a GaAs pyramidal tip (SEM). The magnetic element sketched is placed on the tip sidewall close to its apex. The angle created by sidewalls planes is 72 degrees at the pyramid top. External magnetic field in the horizontal direction (black arrow) can reverse the magnetic moment of the element

the magnetic signal is clearly separated from the topography depicted in Fig. 3 (a). If the bias current flows through the Hall probe, electrostatic forces act onto the MFM tip (case (c)), which causes that atomic forces are not anymore separated from the magnetic and electric forces in the MFM scans. Therefore, the topography defects (holes) seen in Fig. 3 (a) are fully compensated in the MFM image without bias current flowing in the probe (b), but they are clearly visible for non-zero bias current (c), *ie* when electric forces are switched on. Figure 3 (c) then represents a mixture of magnetic, electric and atomic forces.

To summarize this part, the resolution of standard MFM cannot be easily improved by lowering the scanning distance due to increased force mixing in the resulting signal.

2.2 Switching magnetization MFM method

SM-MFM overcomes existing problems of the standard MFM methods (Fig. 4). The tip scans a sample in two passes in the tapping mode with tip magnetization orientation (arrow in the tip) reversed between them. The two traces obtained with opposite tip moments are in one case added and in the second case subtracted. The former then represents atomic forces and the latter the clear magnetic forces only.

The spatial resolution of SM-MFM is increased and the force mixing lowered as compared to the standard MFM techniques. If special tips with very low magnetization are used, the method should be also less invasive than standard one. Such tips have yet to be developed for the SM-MFM technique. In conventional applications MFM tips are prepared by the evaporation or sputtering of magnetic materials onto the standard atomic force microscopy (AFM) tips. The magnetic properties of such tips are defined only roughly and they depend on the coating technique, material and its thickness, etc. Proposed SM-MFM tips must show special magnetic properties:

- The magnetic moment of the tip has to be low and non-invasive within the tapping mode,
- The direction of the magnetic moment has to be reversed easily during scanning,
- The tip must show single-domain state at remanence to keep large stray magnetic field.

Magnetic properties of the SM-MFM tips can be tuned by the shape of the magnetic element located close to the tip apex to achieve high spatial resolution of the SM-MFM technique.

Any magnetic-tip technology and measurement crucially depend on the ability to manufacture a tip with suitable magnetic properties. Our micromagnetic calculations define the optimal shape of a magnetic object that is to be placed on the tip. We show that to lower the switching field of the tip to ~ 3 mT, the magnetic object must be as large as $10\,\mu$m. The technology of the tips suitable for such magnetic objects is based on sharp GaAs pyramids prepared by wet chemical etching [27]. By this procedure, $10\,\mu$m-high pyramids can be fabricated quite easily and reproducibly. We select pyramids with base angle 45 degrees. After etching, epitaxial overgrowth can create atomically flat pyramidal sidewalls that correspond to crystallographic planes of the 110 type [27, 28]. Within the next step, the Py elements of precise shape have to be formed on the tip sidewalls close to their apex using the non-planar lithography [28]. Then a Py layer should be evaporated or sputtered onto the tip and a lift-off technique should be used to finish the Py element on the tip sidewall [29].

Figure 5 shows SEM of the GaAs pyramid (tip) with a sketch of magnetic element, located close to the tip apex. Black lines show pyramid edges, they create a 72 degree angle at the top in the sidewall plane. The black arrow shows the orientation of the external magnetic field that can reverse the tip magnetization.

2.3 Magnetic properties of SM-MFM tips — micromagnetic calculations

Recently, several groups have studied the magnetic properties of Py elements by the micromagnetic calculations and experimentally as well. Most of the studies deal with elliptic and rectangular elements. J. M. García *et al* [30] studied the magnetization process of square-shaped micron-sized Py elements submitted to in-plane magnetic fields, in which high remanence domain structures as well as flux closure configurations were observed. M. Schneider *et al* [31] studied the magnetization reversal of thin submicron Py ellipses and showed strong correlation of the switching field, vortex evolution and annihilation fields with the element shape. Also collective effects in arrays of submicron Py ellipses [32] and Py rings [33] were studied by MFM and modeled by micromagnetic simulations. Serious impact of the edge roughness

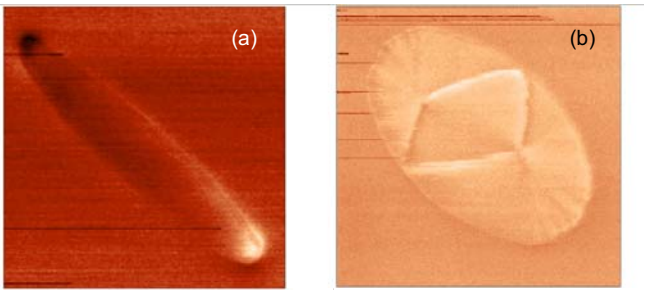

Fig. 6. The difference between single domain state (a) and diamond structure (b) measured on the Py ellipses by MFM. Only single domain state is suitable for probing external magnetic field

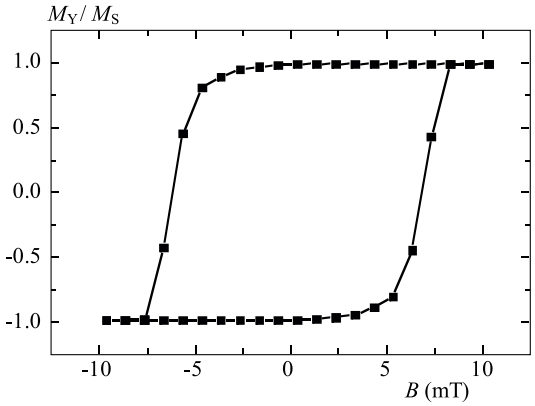

Fig. 7. Hysteresis loop of a single-domain Permalloy element. The simulation shown is for hexagon of length $L = 5000$ nm, width $w = 1500$ nm, and thickness $t = 20$ nm

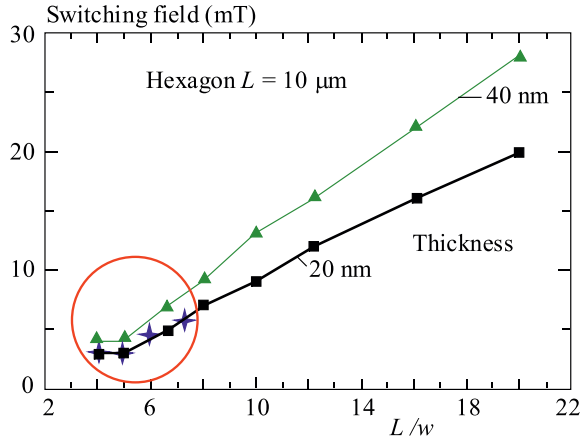

Fig. 8. Comparison of the calculations and experiment for the hexagons ($L = 10\,\mu$m, $t = 20$, 40 nm). Stars are for experimental results

on magnetization switching in Py nanostructures (long stripes) was found and described [34]. The influence of the length-to width ratio and film thickness on switching properties of micrometer-sized elliptical Py elements were studied by Chang *et al* [35].

Based on these calculations and experiments, it can be concluded that the switching fields, vortex evolution and annihilation fields strongly depend on the dimensions and the shape of the Py element explored. Papers mentioned above have investigated ellipses, rings and rectangles only. We have continued the work with other, sharp objects to understand the role of the element dimensions and its aspect ratio on its magnetic properties. We calculated magnetization reversal of the Py elements using micromagnetic simulations, and received switching field H_S versus the element dimensions and shape. The simulations were performed using the software package object oriented micromagnetic framework (OOMMF) [36], which solves the micromagnetic problem using the Landau-Lifshiz-Gilbert (LLG) equation. We used $10\,\text{nm} \times 10\,\text{nm} \times 10\,\text{nm}$ cells (or $5\,\text{nm} \times 5\,\text{nm} \times 5\,\text{nm}$ for smaller elements) for calculations of magnetic state in the elements of the length of $L = 250$ nm – $5\,\mu$m, the width of $w = 10$ nm – $2\,\mu$m, thickness of $t = 20$–50 nm, and for various object shapes. The parameters used for Py are listed below: saturation magnetization $= 8.6 \times 10^5$ (A/m), exchange stiffness $= 1.3 \times 10^5$ (J/m), crystalline anisotropy constant $= 0\,(\text{J/m}^3)$, and damping coefficient $= 0.5$. Throughout the paper the magnetic field is applied along the long axis of the magnetic element simulated.

2.4 Results of the micromagnetic calculations and experiments

We are searching for conditions when Py element is in single-domain magnetic state at remanence. Based on the experiments, the state is achieved for ellipses of length-to-width ratio $L/w > 4$ [34, 37]. The micrometer-scale elongated single-domain magnets are strongly bistable, unlike the two-domain or vortex configurations. Their remanent magnetization always points along the long axis, and if external field of general direction is applied and switched off, it always relaxes into one of two remanent states. Figure 6 shows MFM pictures of two Py ellipses (thickness 20 nm) with ratio $L/w \sim 2$ (left) and $L/w \sim 8$ (right) and at virgin state (without magnetic field applied to the structures before the scans). Our experiments clearly support our calculations as well as calculations and experiments of other groups presented above. The narrower ellipse shows single domain state with magnetization oriented along the long axis.

The wider ellipse shows vortex structure without preferred magnetization orientation, with diamond state created. The magnetic moment of such object is only weakly sensitive to the external magnetic field. Such a diamond state is a stable state of two coupled vortices of opposite orientation. The diamond state increases switching field, and lowers its stray field drastically, which makes such element non-sensitive to external magnetic fields, which is not suitable for SM-MFM tips. We have to avoid such states, and deal with the elements with single-domain states only.

The calculations have shown that the Py objects of hexagonal shape are very perspective for SM-MFM technique because they show single domain state from L/w ratio equal 3 [1]. The typical calculated magnetization loop for the Py hexagon of aspect ratio 3.3 ($L = 5\,\mu$m,

$w = 1500$ nm, $t = 20$ nm) is shown in Fig. 7. In this case, the magnetic flux lines close outside of the sharp apex of the hexagon for each field applied and create strong magnetic stray field that can interact with magnetic samples located close to them, which is needed for SM-MFM tips. Therefore, further calculations were done for hexagons with the apex angle fixed to 72 degrees (corresponding to the AFM pyramid apex).

Calculations of the switching-field H_S of the hexagon on the L/w ratio together with experimental results are shown in Fig. 8. The switching field of the hexagon object is shown as a function of its L/w ratio. All aspect ratios for Py thickness $t = 40$ nm result into higher H_S than for those of thickness $t = 20$ nm, *ie* two branches of the dependence are evident. These two branches are probably connected with the dimensionality of the magnetic system represented by the element. If the element is two-dimensional (2D, $t = 20$ nm), Nel walls are created during switching, and they move easily inside the hexagon. This leads to lower switching field than for thicker elements. If the system is three-dimensional ($t = 40$ nm and more), Bloch walls are created which are better pinned in the system. H_S is increased in comparison with the 2D system and almost equal for all 3D systems at fixed aspect ratio. For wider hexagons the Py thickness does not influence the critical aspect ratio ($L/w = 3.3$), for which the single-domain state is still created. Lowest H_S calculated for hexagon of $L = 10\,\mu$m, $w = 3\,\mu$m and $t = 20$ nm reads $H_S = 3$ mT, which is sufficiently low value, acceptable for the SM-MFM tips.

We have verified the calculated dependence experimentally. For this purpose, we have prepared magnetic Py hexagons using sputtering system AJA ATC-ORION-8E ($L = 10\,\mu$m, w are from 1 m to $3\,\mu$m) using electron beam lithography directly on GaAs semi-insulating substrate. Then we provided MFM scanning experiments in external magnetic field applied in parallel with the long axis of the elements in NTegra SPM system (NT-MDT) with integrated external magnetic field. The experimental results and their comparison with calculations is shown in Fig. 8. The stars represent experimental values for hexagon ($L = 10\,\mu$m, $t = 20$ nm). The figure shows the agreement between the calculations and the experiments. For the hexagons, two branches of the curve are evident, and for wide hexagons a kind of saturation of the switching field is observed in both, calculated and measured data.

3 SUMMARY AND CONCLUSIONS

In this paper we compare the standard MFM technique with the Switching Magnetization Magnetic Force Microscopy (SM-MFM), based on two-pass scanning in tapping mode with reversed tip magnetization between the scans. We show that the second one should increase the MFM resolution and should resolve clear magnetic forces, which is a difficult task due to force mixing and tip invasiveness. For the novel method new MFM tips with easily reversed magnetic moment have to be developed. We have proposed, calculate and experimentally verified the magnetic properties of magnetic hexagons that show low magnetic moment, low switching field (3 mT), and single-domain state at remanence. Tips with such hexagons are suitable for SM-MFM technique and will be realized in the future directly on the tilted sides of pyramidal tips.

Acknowledgement

This work was supported by the Agency of the Ministry of Education, Science, Research and Sport for the EU structural funds for the support of R&D of science in the frame of the activity 2.1, Accessories for laboratory 1 — equipment for metal coating, project Centre of Excellence for New Technologies in Electrical Engineering, ITMS code 26240120011.

References

[1] CAMBEL, V.—ELIÁŠ, P.—GREGUŠOVÁ, D.—MARTAUS, J.—FEDOR, J.—KARAPETROV, G.—NOVOSAD, V.: Magnetic Elements for Switching Magnetization Magnetic Force Microscopy Tips, J. Magnetism Magn. Mater. **322** (2010), 2715–2721.

[2] MARTIN, Y.—WICKRAMASINGHE, H. K.: Magnetic Imaging by Force Microscopy" with 1000Å Resolution, Appl. Phys. Lett. **50** (1987), 1455–1457.

[3] SÁENZ, J. J.—GARCÍA, N.—GRÜTTER, P.—MEYER, E.—HEINZELMANN, H.—WIESENDANGER, R.—ROSENTHALER, L.—HIDBER, H. R.—GÜNTHERODT, H.-J.: Observation of magnetic forces by the atomic force microscope, J. Appl. Phys. **62** (1987), 4293–4295.

[4] RUGAR, D.—MAMIN, H. J.—GUETHNER, P.—LAMBERT, S. E.—STERN, J. E.—MCFAYDEN, I.—YOGI, T.: Magnetic Force Microscopy: General Principles and Application to Longitudinal Recording Media, J. Appl. Phys. **68** (1990), 1169.

[5] ABELMANN, L.—PORTHUN, S.—HAAST, M.—LODDER, C.—MOSER, A.—BEST, M. E.—van SCHENDEL, P. J. A.—STIEFEL, B.—HUG, H. J.—HEYDON, G. P.—FARLEY, A.—HOON, S. R.—PFAFFELHUBER, T.—PROKSCH, R.—BABCOCK, K.: Comparing the Resolution of Magnetic Force Microscopes using the CAMST Reference Samples, J. Magn. Magn. Mater. **190** (1998), 135–147.

[6] PU, A.—THOMSON, D. J.: Sub-Micron Resolution Magnetic Force Microscopy Mapping of Current Paths with Large Probe-to-Sample Separation, Meas. Sci. Technol. **18** (2007), L19–L22.

[7] ALBRECHT, T. R.—GRÜTTER, P.—HORNE, D.—RUGAR, D.: Frequency Modulation Detection using High-Q Cantilevers for Enhanced Force Microscope Sensitivity, J. Appl. Phys. **69** (1991), 668–673.

[8] BABCOCK, K. L.—ELINGS, V. B.—GURLEY, A.—KJOLLER, K.: Method and Apparatus For Obtaining Improved Vertical Metrology Measurements, US Patent No. 5,898,106, Digital Instruments, Santa Barbara, CA (1999).

[9] GUARISCO, D.—NGUY, H.: High Linear Density in Perpendicular Recording, J. Appl. Phys. **93** (2003), 6745–6747.

[10] MARTIN, J. I.—NOGUES, J.—LIU, K.—VICENT, J. L.—SCHULLER, I. K.: Ordered Magnetic Nanostructures: Fabrication and Properties, J. Magn. Magn. Mater. **256** (2003), 449–501.

[11] GEERPURAM, D. N.—MANI, A. S.—BASKARAN, V. S.: A Novel Magnetic Random Access Memory Design using Square

Ring Elements for the Hard Layer, J. Electron. Mater. **33** (2004), 1269–1273.

[12] WOOD, R.: The Feasibility of Magnetic Recording at 1 Terabit per Square, IEEE Trans. Magn. **36** (2000), 36–42.

[13] GRÜTTER, P.—WADAS, A.—MEYER, E.—HEINZELMANN, H.—HIDBER, H.-R.—GRÜNTERODT, H.-J.: High Resolution Magnetic Force Microscopy, J. Vac. Sci. Technol. **A8** (1990), 406–409.

[14] MAMIN, H. J.—RUGAR, D.—STERN, J. E.—FONTANA, R. E.—KASIRAJ, P.: Magnetic Force Microscopy of Thin Permalloy Films, Appl. Phys. Lett. **55** (1989), 318–320.

[15] ENGEL-HERBERT, R.—SCHAADT, D. M.—HESJEDAL, T.: Analytical and Numerical Calculations of the Magnetic Force Microscopy Response: A Comparison, J. Appl. Phys. **99** (2006), 113905.

[16] STREBLECHENKO, D. G.—SCHEINFEIN, M. R.—MANKOS, M.—BABCOCK, K.: Quantitative Magnetometry using Electron Holography: Field Profiles Near Magnetic Force Microscope Tips, IEEE Trans. Magn. **32** (1996), 4124–4129.

[17] SCOTT, J.—MCVITIE, S.—FERRIER, R. P.—GALLAGHER, A.: Electrostatic Charging Artefacts in Lorentz Electron Tomography of MFM Tip Stray Fields, J. Phys. D **34** (2001), 1326–1332.

[18] THIAVILLE, A.—BELLIARD, L.—MAJER, D.—ZELDOV, E.—MILTAT, J.: Measurement of the Stray Field Emanating from Magnetic Force Microscope Tips by Hall Effect Microsensors, J. Appl. Phys. **82** (1997), 3182–3191.

[19] YOSHIDA, N.—YASUTAKE, M.—ARIE, T.—AKITA, S.—NAKAYAMA, Y.: Quantitative Analysis of the Magnetic Properties of Metal-Capped Carbon Nanotube Probe, Jpn. J. Appl. Phys. **41** (2002), 5013–5016.

[20] KURAMOCHI, H.—MANAGO, T.—KOLTSOV, D.—TAKENAKA, M.—IITAKE, M.—AKINAGA, H.: Advantages of CNTMFM Probes in Observation of Domain Walls of Soft Magnetic Materials, Surf. Science **601** (2007), 5289–529.

[21] KOBLISHKA, M. R.—HARTMANN, U.—SULZBACH, T.:
— Improvements of the Lateral Resolution of the MFM Technique, Thin Solid Films **428** (2003), 93–97.
— Resolving Magnetic Nanostructures in the 10-nm Range using MFM at Ambient Conditions, Mat. Sci. Engin. **C23** (2003), 747–751.

[22] HUANG, H. S.—LIN, M. W.—SUN, Y. C.—LIN, L. J.: Improving the Spatial Resolution of a Magnetic Force Microscope Tip via Focused Ion Beam Modification and Magnetic Film Coating, Scr. Mat. **56** (2007), 365–368.

[23] FOLKS, L.—BEST, M. E.—RICE, P. M.—TERRIS, B. D.—WELLER, D.: Perforated Tips for High-Resolution In-Plane Magnetic Force Microscopy, Appl. Phys. Lett. **76** (2000), 909–911.

[24] WOLNY, F.—WEISSKER, U.—MÜHL, T.—LEONHARDT, A.—MENZEL, S.—WINKLER, A.—BÜCHNER, B.: Iron-Filled Carbon Nanotubes as Probes for Magnetic Force Microscopy, J. Appl. Phys. **104** (2008), 064908.

[25] KIRTLEY, J. R.—DENG, Z.—LUAN, L.—YENILMEZ, E.—DAI, H.—MOLER, K. A.: Moment Switching in Nanotube Magnetic Force Probes, Nanotechnology **18** (2007), 465506.

[26] CAMBEL, V.—KARAPETROV, G.—BELKIN, A.—NOVOSAD, V.—ELIÁŠ, P.—GREGUŠOVÁ, D.—FEDOR, J.—KOSTIČ, I.—KÚDELA, R.—ŠOLT YS, J.: Switching Magnetization MFM – Novel Approach to Magnetic Field Imaging, In: Book of abstracts, ISPM (International Scanning Probe Microscopy Conference), Seattle, Washington, USA, June 22–24, (2008).

[27] CAMBEL, V.—GREGUŠOVÁ, D.—KÚDELA, R.: Formation of GaAs Three-Dimensional Objects using AlAs "Facet-Forming" Sacrificial Layer and H_3PO_4, H_2O_2, H_2O based solution, J. Applied Physics **94** (2003), 4643–4648.

[28] 1=ŠOLTÝS, J.—GREGUŠOVÁ, D.—KÚDELA, R.—KUČERA, M.—KOSTIČ, I.—ZAHORAN, M.—CAMBEL, V.: Technology of "Active" Tips for Magnetic and Electric Force Microscopy, In: Book of abstracts, ISPM (International Scanning Probe Microscopy Conference), Seattle, Washington, USA, June 22–24, (2008).

[29] GREGUŠOVÁ, D.—ELI AŠ, P.—ÖSZI, Z.—KÚDELA, R.—ŠOLTÝS, J.—FEDOR, J.—CAMBEL, V.—KOSTIČ, I.: Technology and Properties of a Vector Hall Sensor, Microelectronics J. **37** (2006), 1543–1546.

[30] GARCÍA, J. M.—THIAVILLE, A.—MILTAT, J.—KIRK, K. J.—CHAPMAN, J. N.: MFM Imaging of Patterned Permalloy Elements under an External Applied Field, J. Mag. Mag. Mat. **242** (2002), 1267–1269.

[31] SCHNEIDER, M.—HOFFMANN, H.—ZWECK, J.: Magnetisation Reversal of Thin Submicron Elliptical Permalloy Elements, J. Mag. Mag. Mat. **257** (2003), 1–10.

[32] ZHU, X.—GRÜTTER, P.—METLUSHKO, V.—HAO, Y.—CASTANO, F. J.—ROSS, A.—ILIC, B.—SMITH, H. I.: Construction of Hysteresis Loops of Single Domain Elements and Coupled Permalloy Ring Arrays by Magnetic Force Microscopy, J. Appl. Phys. **93** (2003), 8540–8542.

[33] ZHU, X.—GRÜTTER, P.—METLUSHKO, V.—ILIC, B.: Magnetic Force Microscopy Study of ElectronBeam-Patterned Soft Permalloy Particles: Technique and Magnetization Behavior, Phys. Rev. **B66** (2002), 024423.

[34] BRYAN, M. T.—ATKINSON, D.—COWBURN, R. P.: Experimental Study of the Influence of Edge Roughness on Magnetization Switching in Permalloy Nanostructures, Appl. Phys. Lett. **85** (2004), 3510–3512.

[35] CHANG, C. C.-CHANG, Y. C.—CHUNG, W. S.—WU, J. C.—WIE, Z. H.—LAI, M. F.—CHANG, C. R.: Influences of the Aspect Ratio and Film Thickness on Switching Properties of Elliptical Permalloy Elements, IEEE Trans. on Magnetics **41** (2005), 947–949.

[36] http://math.nist.gov/oommf.

[37] IMRE, A.—CSABA, G.—JI, L.—ORLOV, A.—BERNSTEIN, G. H.—POROD, W.: Majority Logic Gate for Magnetic Quantum-Dot Cellular Automata, Science **311** (2006), 205–207.

Received 14 May 2010

Vladimír Cambel (RNDr, CSc) was born in Bratislava, Slovakia, on May 1956. He received his RNDr and CSc degrees in the Solid State Physics from the Faculty of Mathematics and Physics, Comenius University, Bratislava, in 1980 and 1987, respectively. He is now a scientist at the Institute of Electrical Engineering, Slovak Academy of Sciences, Bratislava. His professional interest is devoted to design, technology, application and tests of novel devices based on III-V heterostructures.

Dagmar Gregušová (RNDr, CSc) was born in 1958 in Partizanske (Slovakia). She received her RNDr degree in solid-state physics from the Faculty of Mathematics, Physics and Informatics, Comenius University and CSc degree from the Slovak Academy of Sciences. Her research activities cover design, technology and analyzes of devices based on III-V and Group III nitrides semiconductors.

Peter Eliáš (Ing) was born in Bratislava, Slovakia, in 1964. He graduated with a Master degree in microelectronics from the Slovak Technical University, Bratislava, in 1988. He works at the Institute of Electrical Engineering of the Slovak Academy of Sciences, where he designs and manufactures micro-and nano-electronic devices based on III-V semiconductors.

Ján Fedor (MSc, PhD) is a scientist at the Institute of Electrical Engineering, Slovak Academy of Sciences. He has finished his master studies at the Faculty of Electrical Engineering, Slovak Technical University in 2001 and he has received PhD degree in Electronics in 2004. His research activities include preparation and characterization of semiconductors and thin metallic films, and their application in microelectronic devices. He has published over 20 scientific papers. At present he is appointed as a deputy director for infrastructure of the Institute of Electrical Engineering.

Ivan Kostič (Dipl-Phys, RNDr) received his Dipl-Phys degree in Physics from Moscow State University, USSR, in 1980. He joined the Laboratory of Electron-beam lithography of the Institute of Technical Cybernetics at the Slovak Academy of Sciences, Bratislava, where he was involved in the research and development of e-beam lithography. Currently he is the leader of the Department of E-beam lithography at the Institute of Informatics of the Slovak Academy of Sciences in Bratislava, where he continues his work on microlithography and microfabrication. His research interests are concentrated on Electron-beam lithography application to microelectronic devices, sensors, microsystems and nanofabrication. He is co-author of more than 60 publications recorded in Current Contents Connect database and more than 110 publications recorded in Web of Science with Conference Proceedings database.

Ján Maňka (Ing, CSc) is a scientist at the Institute of Measurement Science, Slovak Academy of Sciences. He has finished his studies at the Faculty of Electrical Engineering, Slovak Technical University in 1984. He received his CSc degree in measurement science in 1998. His research activities are focused on measurement of extremely weak magnetic fields and its application in material science and biomedicine. He published over 100 scientific papers. He is a leader of the Department of Magnetometry and at present is appointed as a scientific secretary of the Institute of Measurement Science.

Peter Ballo (Prof, Ing, PhD) is a university lecturer and researcher at the Faculty of Electrical Engineering, Slovak University of Technology, Bratislava. He has finished his studies at the Faculty of Electrical Engineering, Slovak University of Technology, Bratislava in 1984. He received a PhD degree in solid state physics in 1993. He was appointed as a professor at the Faculty of Electrical Engineering in 2008. His research activities include molecular dynamics, non linear physics and simulation of defects in semiconductors. He published over 70 scientific papers.

SLOVART G.T.G. s.r.o. GmbH
EXPORT - IMPORT

EXPORT - IMPORT
of periodicals and of non-periodically
printed matters, books and CD-ROMs

Krupinská 4 PO BOX 152, 852 99 Bratislava 5, Slovakia
tel: ++421 2 638 39 472-3, fax: ++421 2 63 839 485
info@slovart-gtg.sk; http://www.slovart-gtg.sk

SLOVART G.T.G. s.r.o. GmbH
EXPORT - IMPORT